Journal of Health Science, **50**(4) 356–365 (2004)

Cardiac Functional Analysis by Electrocardiography, Echocardiography and *in situ* Hemodynamics in Streptozotocin-Induced Diabetic Mice

Yan Li,[a] Yan Gu,[a, b] Ye Song,[a] Li Zhang,[a] Y. James Kang,[a, c, d] Sumanth D. Prabhu,[a, b, e] and Lu Cai*[, a, c]

Department of [a]Medicine, [b]Physiology and Biophysics, [c]Pharmacology and Toxicology, University of Louisville, Louisville, 511 South Floyd Street, MDR 533 Louisville, KY 40202, U.S.A., [d]Jewish Hospital Heart and Lung Institute, and [e]Louisville VA Medical Center, 511 South Floyd Street, MDR 533 Louisville, KY 40202, U.S.A.

(Received February 20, 2004; Accepted March 9, 2004)

Diabetic animal models are used extensively to dissect the mechanisms underlying diabetic cardiomyopathy. For such studies, detection of cardiac dysfunction is critical, and therefore, the present study comparatively examined cardiac function in mice 100 days after strepotozotocin (STZ)-induced diabetes using three complementary techniques: electrocardiography (ECG), echocardiography and left ventricular (LV) hemodynamic analysis. Histological changes were also assessed by periodic acid-Schiff (PAS)-positive materials and Masson's trichrome staining and immunohistochemical staining for type IV collagen. ECG monitoring for 2 hr in diabetic and control mice revealed no abnormality. By echocardiography, diabetic mice showed significant decreases in LV chamber diameter at end-diastole and end-systole but no other abnormalities, as compared to control mice. Hemodynamic evaluation in diabetic mice revealed that although basal parameters of cardiac function were similar to control, β-adrenergic responsiveness was significantly reduced in diabetic mice, indicating a loss of inotropic reserve and early myocardial dysfunction. Histological staining showed mild but significant increases in interstitial fibrosis in diabetic mice, confirming early diabetic cardiomyopathy. These results indicate that despite examination by ECG and resting hemodynamic may not sensitive approaches to reveal early diabetic cardiomyopathy, resting echocardiography and stressing hemodynamic analysis by evaluation of contractile provocation and inotropic reserve are able to uncover the evidence of early subtle mechanical dysfunction.

Key words —— diabetes mellitus, cardiomyopathy, echocardiography, electrocardiography, hemodynamic analysis

INTRODUCTION

The incidence of diabetes mellitus, one of the strongest risk factors for chronic cardiovascular disease, increased significantly worldwide.[1–4] Cardiovascular complications in diabetic patients such as cardiomyopathy are the leading cause of diabetic mortality.[5] Therefore, early diagnosis and prevention of the cardiovascular complications of diabetes are important issues for public health.

Diabetic cardiomyopathy can occur as an independent entity in the absence of chronic vascular disease.[2,5–7] Although there are no diagnostic features for diabetic cardiomyopathy, interstitial accumulation of periodic acid-Schiff (PAS)-positive materials, increased collagen deposition, and interstitial fibrosis have all been commonly noted.[6–8] Such changes in the extracellular matrix can contribute to the diastolic dysfunction observed in patients with diabetes.

To investigate the mechanisms underlying diabetic cardiomyopathy, a variety of animal models has been established.[9] Several methods have been used to detect the early changes in cardiac dysfunction in diabetic animals.[10,11] However, while most methods are feasible in rats or larger animals, vali-

*To whom correspondence should be addressed: Department of Medicine, University of Louisville, Louisville, 511 South Floyd Street, MDR 533 Louisville, KY 40202, U.S.A. Tel.: +1-502-852-5215; Fax: +1-502-852-6904; E-mail: L0cai001@gwise.louisville.edu

dation in mice is lacking. We have previously used hemodynamic analysis to investigate cardiac functional changes in diabetic mice. In that study, we found that significant cardiac dysfunction occurred in diabetic mice 14 days after streptozotocin (STZ)-treatment, and such functional changes were accompanied by histological abnormalities.[12] However, as such hemodynamic analysis requires a terminal study; sequential measurements cannot be performed in the animals. Therefore, noninvasive imaging methods that would allow accurate and serial assessments of structural and functional cardiac changes are of utmost important for transgenic and surgically modified mouse models of diabetes.

Accordingly, in the present study, we comparatively investigated, at 100 days after STZ-treatment, cardiac functional changes in diabetic mice using three approaches: electrocardiography (ECG), echocardiography and left ventricular (LV) hemodynamic analysis. Morphological evaluation was also performed for histological changes seen in diabetic myocardium.

MATERIALS AND METHODS

Diabetic Mouse Model —— FVB mice, originally obtained from Harlan Bioproducts for Science, Inc. (Indianapolis, IN, U.S.A.), were housed in the University of Louisville Research Resources Center at 22°C with a 12-hr light/dark cycle and with free access to rodent chow and tap water. All animal procedures were approved by the Institutional Animal Case and Use Committee, which is certified by the American Association for Accreditation of Laboratory Animal Care. Eight-week old male mice were given a single dose of STZ i.p. (150 mg/kg, Sigma Co., St. Louis, MO, U.S.A.) dissolved in sodium citrate buffer (pH 4.5). Whole-blood was obtained from mouse tail-vein and blood glucose was measured using a SureStep complete blood glucose monitor (LifeScan, Milpitas, CA, U.S.A.). Mice with 12 mmol/l glucose or higher on day 3 after STZ treatment were considered diabetic and were supplied with 1.0 U/kg insulin i.p. daily for up to 2 weeks to avoid acute-phase mortality. The same volume of sodium citrate was given to the mice serving as vehicle controls as described previously.[12,13] Evaluation of cardiac function in diabetic mice 100 days after STZ-treatment was based on the facts that diabetic mice 4 weeks after STZ treatment did not show significant changes by echocardiographic evaluation (a tendency of decreasing LV chamber size was indicated), but other diabetic mice at 12 weeks after diabetic onset showed certain significant echocardiographic abnormalities.[14,15]

Electrocardiography —— ECG was performed on mice anesthetized with sodium pentobarbital (60 mg/kg). The animals are lightly sedated with a single dose of diazepam (i.p., 10 mg/kg) 20 min before the beginning of the recording to obtain stable ECG recordings in unrestrained animals. Needle electrodes were placed subcutaneously in the extremities to obtain Lead II of the ECG. ECG signals were band-pass filtered, amplified, digitized (500 Hz/animal), and recorded by an electrophysiograph. During the recording, the chart speed was set at 10 mm/sec, 25 mm/sec, and 50 mm/sec to allow close examination of the changes in waveforms and for arrhythmia. All analyses were performed on that were obtained full-disclosure 2-hr recordings. QRS complex and T wave were visually confirmed. Each measurement is an average of a 4-sec screen. All complexes on the screen were ensemble averaged using the peak of the QRS as a fiducial point. The QRS complex represents the electrical excitation of the ventricles, which initiates the ventricular contraction (systole) shortly after the Q wave. The R-R interval was determined by averaging individual R-R intervals for all complete cardiac cycles on the screen. The Q-T interval of the signal-averaged complex was then determined manually by placing cursors on the beginning of the QRS and the end of the T wave. Because the Q-T interval was highly correlated with the R-R interval, the QT interval was corrected (Q-Tc) using the formula proposed by Mitchell *et al.*,[16,17] $Q\text{-}Tc = Q\text{-}T/(RR/100)^{1/2}$.

Echocardiography —— Echocardiographic assessment (Toshiba T380 Powervision system) was performed on mice anesthetized with tribromoethanol (0.5 mg/g body weight, by 0.25 ml/g. i.p. injection) in the parasternal long-axis, short-axis, and apical 4-chamber views using a custom-made gel-filled acoustic standoff and a pediatric 7.5-MHz broadband transducer effectively operating at 10-MHz frequency, as described previously.[18] The parasternal views were used to measure anteroposterior internal diameter (D), anterior wall thickness, and posterior wall thickness at end-diastole (ED) and end-systole (ES). Left ventricular systolic function was assessed by fractional shortening (FS = [EDD-ESD]/EDD) and mean velocity of circumferential shortening (Vcf, circ/sec = FS/ejection time) corrected for heart rate (Vcf divided by the square root

of the RR interval in seconds).

Assessment of Left Ventricular Performance ——— General measures of cardiac performance were carried out using *in situ* LV hemodynamic analysis as described previously.[19] Mice were anesthetized using tribromoethanol (0.5 mg/g body weight, by 0.25 ml/g i.p. injection). A midline incision (1–2 cm) in neck external to the trachea was made and the right and left sternohyoid muscles were pulled apart using forceps with serrated tips. A small opening in the trachea was made for the insertion of a PE-100 catheter to ensure a patent airway. The common right carotid artery was isolated, and was tied on the caudal end at the branch point of the internal and external parts to prevent the backflow of blood. The rostra end of the artery was clamped to occlude blood flow from the heart. A small incision was then made in the artery for the insertion of a hand-stretched, fluid-filled PE-50 catheter, which was connected to a transducer and a computer recording system. The catheter was then slowly advanced through the common carotid artery, the ascending aorta, and into the left ventricle. The animal was allowed to stabilize for 20–30 min before recording of the waveform for up to 2 hr.

Isoproterenol was used to generate β-adrenergic stimulation of the LV function. The right femoral vein was cannulated with PE 10 tubing and connected to a Harvard Apparatus/22 microinjecion Pump for the infusion of isoproterenol. After 30–45 min stabilization period, isoproterenol was infused at a rate of 0.02 ml/min (1.6 ng isoproterenol/min/g BW) for 1 min at each time. Myocardial functional changes in response to isoproterenol were recorded immediately after the infusion for 20–30 min at which time myocardial function was recovered to baseline.

Histopathological and Immuonhistochemical Examination by Light Microscopy ——— Heart tissues were cut into 3 mm-thick slices and fixed with 10% neutral formalin overnight. The tissue slices were embedded in paraffin.[20] Tissue sections of 5 μm were stained by PAS and Masson's trichrome and examined with light microscopy as described previously.[21] Type IV collagen (Col IV) was detected using immunohistochemistry method.[21] The primary antibodies were obtained from Santa Cruz Biotechnology (Santa Cruz, CA, U.S.A.). The intensity of PAS, Massonn's and Col IV staining was given a grade from 1 to 5, modified from previous methods,[21] with grade 1 indicting no staining and grade 5 indicating the greatest intensity of staining. A weighted score was then generated to semi-quantify the expression of PAS, Masson's and Col IV in the tissue by multiplying the intensity grade with the proportion of positively staining area (1: 0 to 25% staining; 2: 26–50% staining; 3: 51–75%; and 4: 76–100% staining).

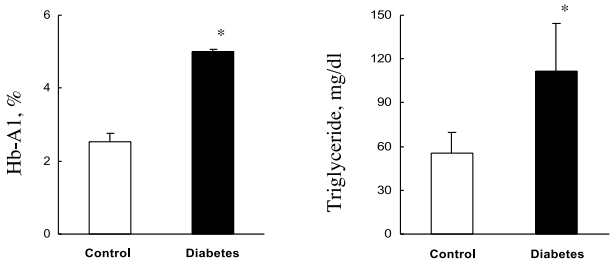

Fig. 1. Diabetic Manifestations

Glycated hemoglobin (Hb-A1) and serum triglyceride in the control and diabetic mice at 100 days after STZ-treatment were measured using corresponding kits from Sigma. $*p < 0.05$ *vs*. control.

Statistical Analysis ——— Data were collected from repeated experiments and are presented as mean ± S.D. Student *t*-test was used for statistical analysis. Differences were considered to be significant at $p < 0.05$.

RESULTS

General Data

A single i.p. injection of 150 mg/kg STZ induced a significant increase in fasting whole-blood glucose levels (>12 mmol/l) in the mice from day 3 to 100 after STZ-treatment. Animals with hyperglycemia persisting for 100 days after STZ-treatment were used in this experiment. Eight mice for each group were included, but 2 diabetic mice died at 1 and 2 months. The diabetic mice showed a significant increase in glycated hemoglobin (Hb-A) and serum triglyceride levels (Fig. 1). Baseline body weight (day 0) was not different between control and diabetic mice, but significantly decreased in the diabetic mice 100 days after STZ-treatment (Table 1). Heart weights in diabetic mice were lower than controls, although ratios of heart weight to body weight were increased due to the significant decrease in body weight (Table 1). Both kidney weight and ratio of kidney weight to body weight increased in diabetic mice, indicating significant renal injury (Table 1). Since we have demonstrated decreased spermatogenesis along with a marked decrease in

Table 1. Body and Organ Weight (gram)[a)]

	Control	Diabetes	*p*-values
Body weight (BW)			
Day 0	25.9 ± 1.9	25.8 ± 3.1	
Day 100	31.4 ± 3.1	27.1 ± 4.1	0.04
Heart weight (HW)	0.14 ± 0.02	0.12 ± 0.01	0.13
Ratio of HW/BW	0.43 ± 0.03	0.45 ± 0.04	0.56
Kidney weight (KW)	0.25 ± 0.01	0.28 ± 0.04	0.04
Ratio of KW/BW	0.79 ± 0.08	1.03 ± 0.18	0.01
Testes weight (TW)	0.36 ± 0.04	0.26 ± 0.09	0.01
Ratio of TW/BW	0.30 ± 0.05	0.24 ± 0.07	0.12

a) Eight mice were included for each (control and diabetes) group in beginning of the experiment, but two diabetic mice died at one and two month after STZ-treatment as described in the text.

testes weight in the diabetic rats,[22)] we also measured testes weight as an endpoint of diabetic manifestations, which decreased significantly (although the ratios of testes weight to body weight increased due to significant loss of body weight in diabetic group). These findings indicate significant organ damage in diabetic mice 100 days after STZ-treatment.

Electrocardiographic Evaluation of Diabetic Mice

Eight control and six diabetic mice were evaluated by ECG for electrophysiological changes. Representative ECGs from control and diabetic mice are presented in Fig. 2A. The electrocardiogram of an adult mouse differs considerably from that of humans, with the most notable difference being the absence of an identifiable S-T segment. Instead, in lead II, there is an early-peaking, upright T wave that is merged with the QRS. Analysis indicated the normal QRS complex (8.43 ± 0.13 ms for control *vs*. 8.42 ± 0.21 ms for diabetes) and Q-Tc interval (50.40 ± 0.50 ms for saline control *vs*. 50.48 ± 0.39 ms for diabetes), and the absence of T wave shifts in both normal and diabetic mice. No ventricular premature beat was found during a 2-hr observation period in each mouse from both control and diabetic groups.

Echocardiographic Evaluation of Diabetic Mice

Echocardiography revealed reduced LV chamber size evidenced by smaller LVEDD and LVEDV, and LVESD and LVESV (Table 2), but without significant changes in absolute or relative wall thickness as well as LV mass. A representative result indicating the decrease in LVEDD and LVESD in diabetic mice as compared to control mice was presented in Fig. 2B. No hypertrophic remodeling was observed. Additionally, LV systolic function mea-

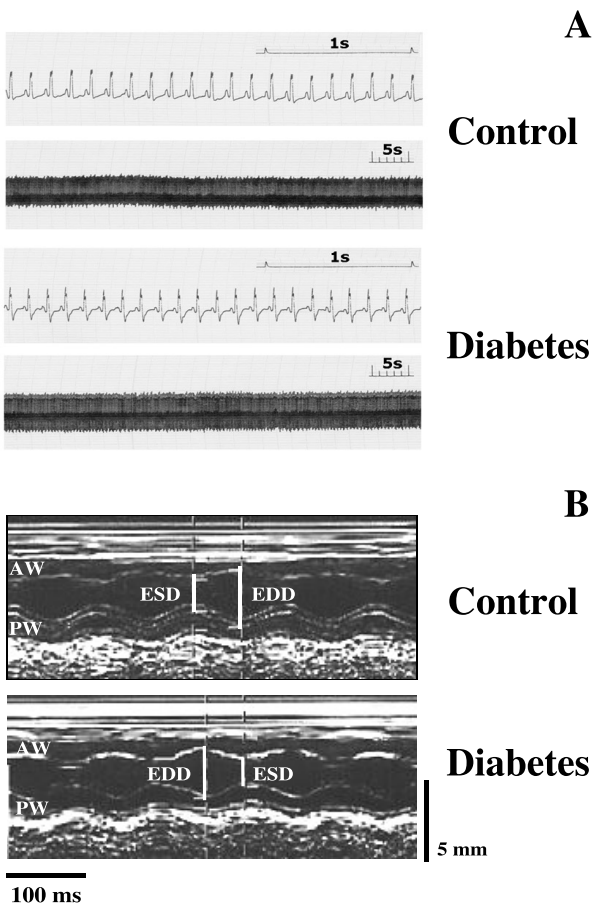

Fig. 2. Representative Measurements of Cardiac Function by ECG (A) and Echocardiography (B) in Control and Diabetic Mice 100 days after STZ-Treatment

Table 2. Measurements of Baseline Cardiac Function by Echocardiography

Parameters	Control	Diabetes	*p*-values
Heart rate, beats/min	517 ± 16	540 ± 22	0.43
LVEDD, mm	3.9 ± 0.1	3.5 ± 0.2	0.07
LVESD, mm	2.2 ± 0.1	1.9 ± 0.1	0.04
SWT, mm	0.88 ± 0.05	0.87 ± 0.07	0.93
PWT, mm	0.91 ± 0.03	0.85 ± 0.05	0.39
RWT	0.46 ± 0.02	0.50 ± 0.05	0.51
Vcfc, circ/sec	24.3 ± 1.8	28.7 ± 2.2	0.16
FS	0.43 ± 0.02	0.47 ± 0.02	0.12
LV mass, mg	130.4 ± 8.2	105.0 ± 12.0	0.12
EDV, Cube	58.6 ± 3.7	43.7 ± 1.0	0.05
ESV, Cube	11.6 ± 1.6	6.9 ± 1.0	0.03

LVEDD and LVESD, left ventricular end-diastolic or end-systolic diameter; SWT, septal wall thickness; PWT, posterior wall thickness; RWT, relative wall thickness = (SWT+PWT)/LVEDD; and Vcfc, corrected Vcf, *i.e.* mean velocity of circumferential shortening (Vcf, circ/sec = FS/ejection time) divided by the square root of the RR interval. Data are the mean ± S.D.

Table 3. Hemodynamic Analysis

Parameters	Control	Diabetes	*p*-values
Measurements in aorta			
Heart rate	407.4 ± 46.8	449.9 ± 67	0.3
Systolic blood pressure, mmHg	91.2 ± 5.2	108.8 ± 11.3	0.02
Diastolic blood pressure, mmHg	63.7 ± 6.2	75.4 ± 11.7	0.15
Measurements in left ventricle			
Heart rate	419.1 ± 81.0	461.4 ± 16.0	0.42
LVPSP, mmHg	103.2 ± 8.9	123.7 ± 12.7	0.03
LVEDP, mmHg	1.7 ± 3.4	2.9 ± 2.7	0.60
LVMDP, mmHg	−6.6 ± 4.9	−11.1 ± 8.1	0.33
dP/dt max, mmHg/s	7482.8 ± 1886.5	7832.3 ± 1220.1	0.78
DCON, msec	39.4 ± 10.3	35.0 ± 5.3	0.52
Tau, msec	20.2 ± 7.8	21.0 ± 6.6	0.89
1/2 R, msec	41.4 ± 13.4	40.0 ± 6.7	0.88
NdP/dt min, mmHg/s	5271.7 ± 1277.1	6030.2 ± 1086.8	0.41
DREL, msec	60.5 ± 15.1	60.9 ± 3.6	0.97

LVPSP, LV peak systolic pressure; LVEDP, LV end-diastolic pressure; LVMDP, LV minimum diastolic pressure; dP/dt max, maximum rate of rise in intraventricular pressure during ventricular contraction; DCON, duration of contraction; Tau, time constant of the best-fit exponential pressure decay from the pressure at dP/dt max to a positive pressure above the previous LVEDP by 10 mmHg; time constant; 1/2R: duration of 1/2 relaxation; dP/dt min, maximum rate of decrease in intraventricular pressure during the isovolumetric relaxation; DREL: duration of relaxation. Values are means ± S.D.

sured by fractional shortening and mean velocity of circumferential shortening (FS and Vcf) was unchanged.

Hemodynamic Analysis of Diabetic Mice

Resting hemodynamic analysis revealed significant increase in systolic blood pressure and accordingly LV peak systolic pressure (LVPSP) without other differences between diabetic and control mice, as shown in (Table 3). In response to isoproterenol stimulation, no difference for the increased heart rates was seen between control and diabetes, but LVEDP significantly increased in diabetic mice (about 10 folds relative to diabetic baseline) as compared to control mice although there was no significant difference due to individual variation (Fig. 3A). However, the values of +dP/dt max, a measurement of the mechanical ability of the heart to generate

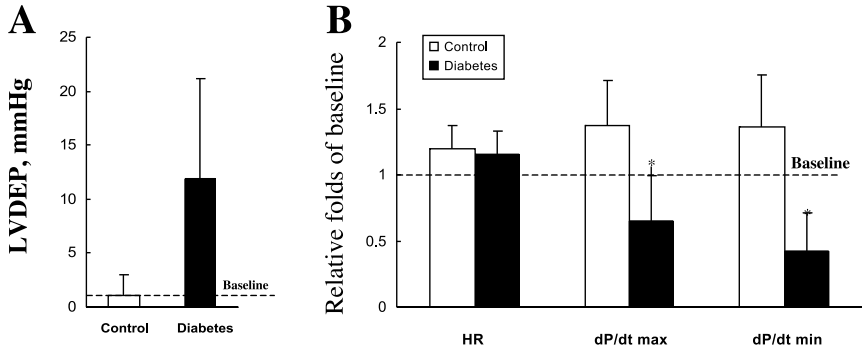

Fig. 3. Hemodynamic Changes in Response to Isoproterenol Stimulation

Left ventricular end diastolic pressure (A), and heart rate (HR), maximum dP/dt and minimum dP/dt were compared by baseline (indicated by horizontal dash line) and that in response to isoproterenol stimulation (B) were measured, as described in MATERIALS AND METHODS. $*p < 0.05$ *vs.* corresponding control groups.

force for ejection of blood from the LV, were markedly reduced in the diabetic mice compared to control after isoproterenol stimulation. Correspondingly, the value of –dP/dt min was also significantly decreased in the diabetic mice (Fig. 3B). The loss of inotropic reserve uncovered during β-adrenergic stimulation suggests early cardiac dysfunction in diabetic mice 100 days after STZ.

Histological Examination of the Hearts of Diabetic Mice

Histological examination, by light microscopy using hematoxylin and eosin staining, of ventricular tissue sections revealed the presence of myocardial disarray in diabetic mice (data not shown). There were increased PAS-positive materials and Masson's trichrome staining in diabetic myocardium as compared to control (Fig. 4). Col IV staining intensity was also increased in diabetic myocardium as compared to controls (Fig. 4).

DISCUSSION

The results of this study demonstrated that: Prolonged (2-hr) ECG monitoring does not reveal any electrophysiological abnormalities in STZ-induced diabetic mice, diabetes is associated with reduced chamber size by echocardiography, but no hypertrophy or baseline mechanical dysfunction, and diabetic mice display no alteration in resting hemodynamics, but have a loss of inotropic reserve, with reduced β-adrenergic responsiveness. These alterations indicate early evidence of myocardial dysfunction, which was confirmed by histopathological evidence of increased PAS-positive materials, Masson's trichrome and Col IV staining in diabetic myocardium.

Autonomic neuropathy is a common complication of both type 1 and 2 diabetes mellitus. QT interval prolongation and QT dispersion, which is defined as the difference between the longest corrected QT interval and the shortest corrected QT interval, are important manifestations of diabetic neuropathy and have been used to screen diabetic patients at risk for sudden cardiac death.[23–25] Using ECG to evaluate cardiac function of STZ-induced diabetes in the rat, spontaneous arrhythmic activity (lasted only a few seconds) and prolonged QT interval (QT interval corrected for heart rate) were observed, but not earlier than 16 weeks after STZ treatment.[26] Compared to rat model, only a few studies used ECG assessments for cardiac dysfunction in other mouse models,[16,27,28] in which no prolonged QT interval was noted even though other ECG abnormalities were observed. In addition, whether prolonged QT interval directly correlates to and predicts arrhythmia risk arrhythmia was also questioned in other non-diabetic cardiomyopathy mouse model.[29] We have successfully applied the ECG to evaluate the effect of air pollute on cardiac dysfunction in the rat models with acute myocardial infarction.[17] In the present study using mouse diabetic model, however, ECG evaluation did not reveal any abnormality in diabetic group as compared to control. This may be secondary to: the duration of diabetes in the present study (100 days) may not produce significant cardiac neuropathic changes, 2-hr ECG observation may be too brief to uncover such abnormalities; and the use of ECG, especially QT interval, for the evaluation of cardiomyopathy may be adequate in mouse model.

In the present study, we found that diabetes was

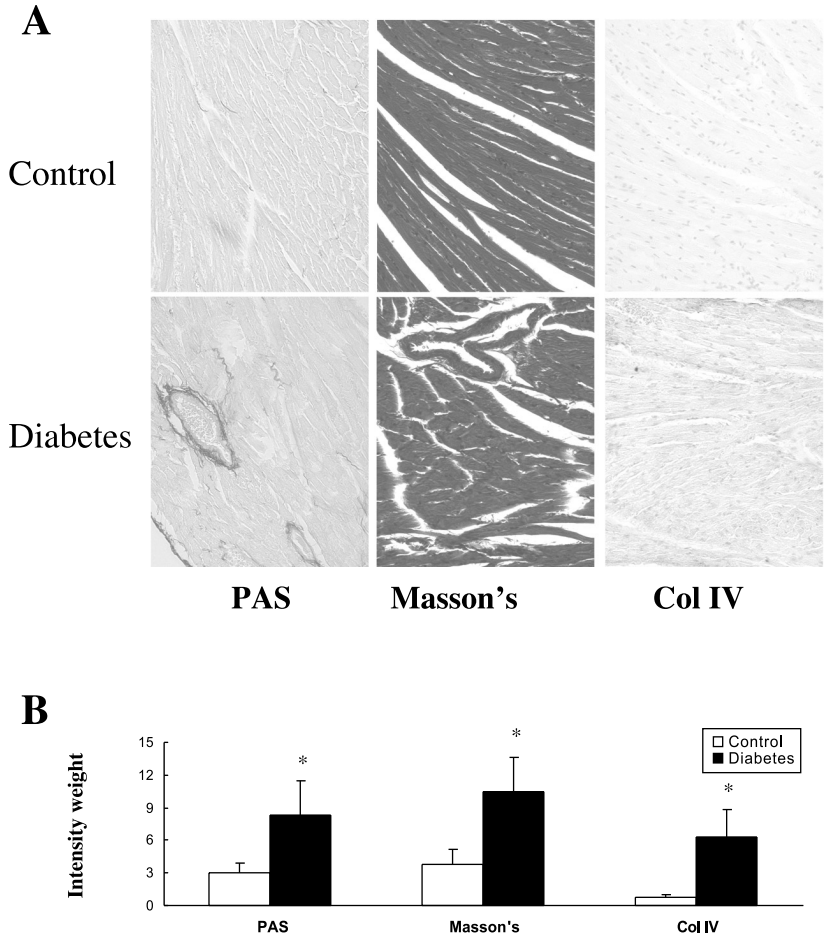

Fig. 4. Histopathological and Immunohistochemical Staining

PAS-positive materials, Masson's trichrome staining and Col IV immunohistochemical staining were performed in the heart tissues from control and diabetic mice 100 days after STZ-treatment. $*p < 0.05$ *vs.* corresponding control groups. Scoring standards were described in MATERIALS AND METHODS.

associated with reduced chamber size, shown by decreases in LVEDD or LVEDV and LVESD or LVESV (Table 2). A few studies used echocardiography to evaluate cardiac dysfunction in diabetic mouse models including both type 1[15,30] and type 2 diabetes.[14,31,32] In regarding to type 1 diabetes, our results are consistent with study of Shiomi *et al.*[30] and inconsistent with the study of Nielsen *et al.*[15] which revealed a slight increase in LVEDD and LVESD in diabetic mice 3 months after STZ treatment. These discrepancies may be due to the use of anesthesia,[10,33] the duration of diabetes[34] and, perhaps more importantly, the type of diabetic models. For instance, in the studies of Shiome *et al.*[30] and the present study, tribromoethanol/amylene hydrate (Avertin) was used, and in the study of Nielsen *et al.*[15] hypnorm/diazepam (1 : 1) was used, while in other studies,[14,32] no anesthesia was used. In addition, we examined a single-high-dose STZ-induced type 1 diabetic model, which is same as that in the study by Shiome *et al.*,[30] whereas others used either type 2 diabetes (db/db mice or high-fat-induced diabetes)[14,31,32] or type-1 diabetes induced by multiple-low dose of STZ.[15] Compared to single-high dose of STZ, diabetes induced by multiple-low doses of STZ has significantly different mechanisms for the development of diabetes.[35,36]

Single-high-dose STZ induces a sudden and very high levels of blood glucose, which may result in hyperosmotic shrinking of ventricular myocytes.[37] We has demonstrated that exposure of cardiac cells to hyperglycemia caused a significant increase in apoptotic cell death,[13] which supports the evidence of cardiac cell loss in response to sudden increase in blood glucose in animals.[38,39] In addition, insulin which is deficient in type-1 diabetes is an effective cardioprotective factor against cell loss caused by a variety of oxidative stimuli[40] and mice with null of

the insulin-like growth receptor gene showed a reduced heart size.[41] These factors may explain the decreases in heart weight (Table 1) and chamber size observed by the present (Table 2, Fig. 2B) and other studies.[28,38]

By hemodynamic examination, no significant differences in basal mechanical parameters were observed between diabetic and control mice. This conflicts with previous studies[12,38] in which LVEDP was increased in diabetic mice 14 days and diabetic rats 28 day after STZ treatment. One explanation for this difference may be related to the reversibility of a compensation for early cardiac dysfunction. As the development of diabetes progresses to a subacute phase (100 days after STZ treatment), the myocardial response to these diabetic alterations may mask the subtle cardiac mechanical dysfunction. However, the diabetic heart does display a loss of inotropic reserve in response to β-adrenergic stress (Fig. 3), and underscores the need for stress-provocation to elicit cardiac dysfunction in diabetic mice. These changes may become more apparent with longer duration of disease, which will be explored further in future studies.

Limitations of the present study are: small group of diabetic animals; too short period of hyperglycemia which may cause insignificant abnormalities by echocardiography and resting hemodynamic analysis; and echocardiographic evaluation of diabetic mice without combination of treadmill exercise, which may enhance the sensitivity of echocardiographic evaluation of subtle cardiac dysfunction. Although these shortages are required to be overcome in the future studies, the present study remains to provide importantly comparative information in the same mice for functional evaluation of diabetic cardiomyopathy. These results suggest that a comprehensive mechanical assessment incorporating inotropic stimulation may be the most useful approach to detection of diabetic cardiomyopathy.

Acknowledgements This work was supported in part by grants JHF 010808 from the Jewish Hospital Foundation, PM020187 from the Philip Morris USA, Inc., ADA020667 from the American Diabetes Association to LC, by grants HL63760 and HL59225 from the National Institutes of Health to YJK, and by grants NIH P01 ESO11860-01A1 from the National Institutes of Health and a Veterans Administration Merit grant to SDP. YJK and SDP are a Distinguished University Scholar and University Scholar, respectively, of the University of Louisville.

REFERENCES

1) Centers for Disease Control and Prevention (CDC) (2003) Prevalence of diabetes and impaired fasting glucose in adults — United States, 1999–2000. *MMWR Morb. Mortal. Wkly Rep.*, **52**, 833–837.
2) Engelgau, M. M., Narayan, K. M., Saaddine, J. B. and Vinicor, F. (2003) Addressing the burden of diabetes in the 21st century: better care and primary prevention. *J. Am. Soc. Nephrol.*, **14**(Suppl. 2), S88–S91.
3) Jaber, L. A., Brown, M. B., Hammad, A., Nowak, S. N., Zhu, Q., Ghafoor, A. and Herman, W. H. (2003) Epidemiology of diabetes among Arab Americans. *Diabetes Care*, **26**, 308–313.
4) Gu, D., Reynolds, K., Duan, X., Xin, X., Chen, J., Wu, X., Mo, J., Whelton, P. K., He, J. and InterASIA Collaborative Group (2003) Prevalence of diabetes and impaired fasting glucose in the Chinese adult population: International Collaborative Study of Cardiovascular Disease in Asia (InterASIA). *Diabetologia*, **46**, 1190–1198.
5) Cai, L. and Kang, Y. J. (2001) Oxidative stress and diabetic cardiomyopathy: a brief review. *Cardiovasc. Toxicol.*, **1**, 181–193.
6) Regan, T. J., Lyons, M. M., Ahmed, S. S., Levinson, G. E., Oldewurtel, H. A., Ahmad, M. R. and Haider, B. (1977) Evidence for cardiomyopathy in familial diabetes mellitus. *J. Clin. Invest.*, **60**, 884–899.
7) Factor, S. M., Minase, T. and Sonnenblick, E. H. (1980) Clinical and morphological features of human hypertensive-diabetic cardiomyopathy. *Am. Heart J.*, **99**, 446–458.
8) van Hoeven, K. H. and Factor, S. M. (1990) A comparison of the pathological spectrum of hypertensive, diabetic, and hypertensive-diabetic heart disease. *Circulation*, **82**, 848–855.
9) Shafrir, E. (1990) Diabetes in animals, In *Diabetes Mellitus: Theory and Practice* (Rifkin, H. and Porte, D., Jr., Eds.), 4th edition, Elsevier, New York, pp. 299–340.
10) Chaves, A. A., Weinstein, D. M. and Bauer, J. A. (2001) Non-invasive echocardiographic studies in mice: influence of anesthetic regimen. *Life Sci.*, **69**, 213–222.
11) Chu, V., Otero, J. M., Lopez, O., Morgan, J. P., Amende, I. and Hampton, T. G. (2001) Method for non-invasively recording electrocardiograms in conscious mice. *BMC Physiol.*, **1**, 6–8.
12) Cai, L., Wang, J., Sun, X., Li, Y., Wang, L., Zhou, Z. and Kang, Y. J. (2004) Suppression of superoxide accumulation is involved in metalltothionein prevention of diabetic cardiomyopathy. *Diabetes*, submitted.
13) Cai, L., Li, W., Wang, G., Guo, L., Jiang, Y. and

Kang, Y. J. (2002) Hyperglycemia-induced apoptosis in mouse myocardium: mitochondrial cytochrome c-mediated caspase-3 activation pathway. *Diabetes*, **51**, 1938–1948.

14) Semeniuk, L. M., Kryski, A. J. and Severson, D. L. (2002) Echocardiographic assessment of cardiac function in diabetic db/db and transgenic db/db-hGLUT4 mice. *Am. J. Physiol. Heart Circ. Physiol.*, **283**, H976–H982.
15) Nielsen, L. B., Bartels, E. D. and Bollano, E. (2002) Overexpression of apolipoprotein B in the heart impedes cardiac triglyceride accumulation and development of cardiac dysfunction in diabetic mice. *J. Biol. Chem.*, **277**, 27014–27020.
16) Mitchell, G. F., Jeron, A. and Koren, G. (1998) Measurement of heart rate and Q-T interval in the conscious mouse. *Am. J. Physiol.*, **274**, H747–H751.
17) Kang, Y. J., Li, Y., Zhou, Z., Roberts, A. M., Cai, L., Myers, S. R., Wang, L. and Schuchke, D. A. (2002) Elevation of serum endothelins and cardiotoxicity induced by particulate matter (PM2.5) in rats with acute myocardial infarction. *Cardiovasc. Toxicol.*, **2**, 253–261.
18) Black, R. G., Jr., Guo, Y., Ge, Z. D., Murphree, S. S., Prabhu, S. D., Jones, W. K., Bolli, R. and Auchampach, J. A. (2002) Gene dosage-dependent effects of cardiac-specific overexpression of the A3 adenosine receptor. *Circ. Res.*, **91**, 165–172.
19) Li, Y., Sun, X., Wang, L., Zhou, Z. and Kang, Y. J. (2002) Myocardial toxicity of arsenic trioxide in a mouse model. *Cardiovasc. Toxicol.*, **2**, 63–73.
20) Song, Y., Song, Z., Zhang, L., McClain, C. J., Kang, Y. J. and Cai, L. (2003) Diabetes enhances lipopolysaccharide-induced cardiac toxicity in the mouse model. *Cardiovasc. Toxicol.*, **3**, 363–372.
21) Song, Y., Li, C. and Cai, L. (2004) Fluvastatin prevents nephropathy likely through suppression of connective tissue growth factor-mediated extracellular matrix accumulation. *Exp. Mol. Pathol.*, **76**, 66–75.
22) Cai, L., Chen, S., Evans, T., Cherian, M. G. and Chakrabarti, S. (2002) Endothelin-1-mediated alteration of metallothionein and trace metals in the liver and kidneys of chronically diabetic rats. *Int. J. Exp. Diabetes Res.*, **3**, 193–198.
23) Kahn, J. K., Sisson, J. C. and Vinik, A. I. (1987) QT interval prolongation and sudden cardiac death in diabetic autonomic neuropathy. *J. Clin. Endocrinol. Metab.*, **64**, 751–754.
24) Veglio, M., Chinaglia, A. and Cavallo Perin, P. (2000) The clinical utility of QT interval assessment in diabetes. *Diabetes Nutr. Metab.*, **13**, 356–365.
25) Wei, K., Dorian, P., Newman, D. and Langer, A. (1995) Association between QT dispersion and autonomic dysfunction in patients with diabetes mellitus. *J. Am. Coll. Cardiol.*, **26**, 859–863.
26) Navaratnam, S. and Khatter, J. C. (1989) Influence of the diabetic state on digitalis-induced cardiac arrhythmias in rat. *Arch. Int. Pharmacodyn. Ther.*, **301**, 151–164.
27) Burcelin, R., Kamohara, S., Li, J., Tannenbaum, G. S., Charron, M. J. and Friedman, J. M. (1999) Acute intravenous leptin infusion increases glucose turnover but not skeletal muscle glucose uptake in ob/ob mice. *Diabetes*, **48**, 1264–1269.
28) Elliott, J. F., Liu, J., Yuan, Z. N., Bautista-Lopez, N., Wallbank, S. L., Suzuki, K., Rayner, D., Nation, P., Robertson, M. A., Liu, G. and Kavanagh, K. M. (2003) Autoimmune cardiomyopathy and heart block develop spontaneously in HLA-DQ8 transgenic IAbeta knockout NOD mice. *Proc. Natl. Acad. Sci. U.S.A.*, **100**, 13447–13452.
29) Bevilacqua, L. M., Maguire, C. T., Seidman, J. G., Seidman, C. E. and Berul, C. I. (1999) QT dispersion in alpha-myosin heavy-chain familial hypertrophic cardiomyopathy mice. *Pediatr. Res.*, **45**, 643–647.
30) Shiomi, T., Tsutsui, H., Ikeuchi, M., Matsusaka, H., Hayashidani, S., Suematsu, N., Wen, J., Kubota, T. and Takeshita, A. (2003) Streptozotocin-induced hyperglycemia exacerbates left ventricular remodeling and failure after experimental myocardial infarction. *J. Am. Coll. Cardiol.*, **42**, 165–172.
31) Finck, B. N., Han, X., Courtois, M., Aimond, F., Nerbonne, J. M., Kovacs, A., Gross, R. W. and Kelly, D. P. (2003) A critical role for PPARalpha-mediated lipotoxicity in the pathogenesis of diabetic cardiomyopathy: modulation by dietary fat content. *Proc. Natl. Acad. Sci. U.S.A.*, **100**, 1226–1231.
32) Carley, A. N., Semeniuk, L. M., Shimoni, Y., Aasum, E., Larsen, T. S., Berger, J. P. and Severson, D. L. (2004) Treatment of type 2 diabetic db/db mice with a novel PPAR {gamma} agonist improves cardiac metabolism but not contractile function. *Am. J. Physiol. Endocrinol. Metab.*, **286**, E449–E455.
33) Roth, D. M., Swaney, J. S., Dalton, N. D., Gilpin, E. A. and Ross, J., Jr. (2002) Impact of anesthesia on cardiac function during echocardiography in mice. *Am. J. Physiol. Heart Circ. Physiol.*, **282**, H2134–H2140.
34) Semeniuk, L. M., Severson, D. L., Kryski, A. J., Swirp, S. L., Molkentin, J. D. and Duff, H. J. (2003) Time-dependent systolic and diastolic function in mice overexpressing calcineurin. *Am. J. Physiol. Heart Circ. Physiol.*, **284**, H425–H430.
35) McEvoy, R. C., Andersson, J., Sandler, S. and Hellerstrom, C. (1984) Multiple low-dose streptozotocin-induced diabetes in the mouse. Evidence

for stimulation of a cytotoxic cellular immune response against an insulin-producing beta cell line. *J. Clin. Invest.*, **74**, 715–722.

36) Lukic, M. L., Stosic-Grujicic, S. and Shahin, A. (1998) Effector mechanisms in low-dose streptozotocin-induced diabetes. *Dev. Immunol.*, **6**, 119–128.

37) Howarth, F. C., Qureshi, M. A. and White, E. (2002) Effects of hyperosmotic shrinking on ventricular myocyte shortening and intracellular Ca(2+) in streptozotocin-induced diabetic rats. *Pflugers Arch.*, **444**, 446–451.

38) Fiordaliso, F., Li, B., Latini, R., Sonnenblick, E. H., Anversa, P., Leri, A. and Kajstura, J. (2000) Myocyte death in streptozotocin-induced diabetes in rats in angiotensin II-dependent. *Lab. Invest.*, **80**, 513–527.

39) Ceriello, A., Quagliaro, L., D'Amico, M., Di Filippo, C., Marfella, R., Nappo, F., Berrino, L., Rossi, F. and Giugliano, D. (2002) Acute hyperglycemia induces nitrotyrosine formation and apoptosis in perfused heart from rat. *Diabetes*, **51**, 1076–1082.

40) Suzuki, Y. J. (2003) Growth factor signaling for cardioprotection against oxidative stress-induced apoptosis. *Antioxid. Redox Signal.*, **5**, 741–749.

41) Belke, D. D., Betuing, S., Tuttle, M. J., Graveleau, C., Young, M. E., Pham, M., Zhang, D., Cooksey, R. C., McClain, D. A., Litwin, S. E., Taegtmeyer, H., Severson, D., Kahn, C. R. and Abel, E. D. (2002) Insulin signaling coordinately regulates cardiac size, metabolism, and contractile protein isoform expression. *J. Clin. Invest.*, **109**, 629–639.